Neuron, Vol. 29, 757–767, March, 2001, Copyright ©2001 by Cell Press

Eye Movements Modulate Visual Receptive Fields of V4 Neurons

Andreas S. Tolias,*§‖ Tirin Moore,*#
Stelios M. Smirnakis,† Edward J. Tehovnik,*
Athanassios G. Siapas,*‡ and Peter H. Schiller*
*Department of Brain and
Cognitive Sciences
Massachusetts Institute of Technology
Building E25, Room 634
Cambridge, Massachusetts 02139
†Department of Neurology
Massachusetts General Hospital and
Brigham and Women's Hospital
Harvard Medical School
ACC 835, 32 Fruit Street
Boston, Massachusetts 02114
‡Center for Learning and Memory
Massachusetts Institute of Technology
Cambridge, Massachusetts 02139

Summary

The receptive field, defined as the spatiotemporal selectivity of neurons to sensory stimuli, is central to our understanding of the neuronal mechanisms of perception. However, despite the fact that eye movements are critical during normal vision, the influence of eye movements on the structure of receptive fields has never been characterized. Here, we map the receptive fields of macaque area V4 neurons during saccadic eye movements and find that receptive fields are remarkably dynamic. Specifically, before the initiation of a saccadic eye movement, receptive fields shrink and shift towards the saccade target. These spatiotemporal dynamics may enhance information processing of relevant stimuli during the scanning of a visual scene, thereby assisting the selection of saccade targets and accelerating the analysis of the visual scene during free viewing.

Introduction

The concept of the neuronal receptive field, i.e., the spatiotemporal sensitivity to sensory stimulation, is instrumental to our current understanding of the neuronal mechanisms that underlie sensory processing in the brain (Hartline, 1940). Within the visual system of the macaque monkey, neuronal receptive fields have been identified in many cortical regions including the striate cortex and areas of the temporal, parietal, and frontal lobes (Wurtz, 1969; Dubner and Zeki, 1971; Desimone and Gross, 1979; Andersen and Mountcastle, 1983; Suzuki and Azuma, 1983; Blatt et al., 1990; Boussaoud et al., 1991; Hikosaka, 1998; Rainer et al., 1998). Until now, the receptive field properties of visual neurons have been predominantly studied during anesthesia or active fixation. Primates, however, analyze the visual scene dynamically by performing a series of rapid scanning eye movements known as saccades (Yarbus, 1967; Carpenter, 1988). The responses of many neurons in the cerebral cortex are in fact modulated around the time of visually guided saccades. Such modulation has been reported for neurons in the frontal eye fields (Wurtz and Mohler, 1976), the lateral intraparietal area (Robinson et al., 1978), the prefrontal cortex (Boch and Goldberg, 1989), and area V4 (Fischer and Boch, 1981a, 1981b; A. S. Tolias et al., 1997, Soc. Neurosci., abstract; Moore et al., 1998; Moore, 1999). Specifically, the activity of neurons to stimuli presented in their classical receptive field (CRF) is enhanced prior to the execution of saccades when these stimuli are targets for eye movements. Yet, the effect of eye movements on the structure of the receptive field itself has never been measured.

To determine the influence of eye movements on the structure of the receptive field, we developed a novel behavioral task in order to map the receptive fields of extrastriate area V4 neurons during saccade execution. After the monkey acquired fixation, a visual stimulus (probe) was presented that persisted on the monitor for the duration of the trial. Subsequently, a saccade target appeared and the monkey executed a saccade (Figure 1a). By varying the location of the probe and the saccade target from trial to trial, we were able to map neuronal receptive fields for different saccade vectors. Our experimental paradigm also enabled us to analyze the dynamics of neuronal receptive fields during the execution of saccadic eye movements. We found that prior to the initiation of saccadic eye movements, receptive fields shrink and shift toward the saccade target.

Results

Spatiotemporal Sensitivity

We measured the spatiotemporal sensitivity of cells in V4 during the execution of visually guided saccadic eye movements using a *persistent* probe (Figure 1). After the monkey acquired fixation, the probe appeared at a location chosen randomly from a predetermined set of positions and remained on the screen until the end of the trial when the animal was rewarded. Three hundred to one thousand millseconds after the onset of the probe, the saccade target appeared at one of a number of possible locations. Upon saccade target onset, the fixation target was extinguished, and the monkey was rewarded for foveating the saccade target. The probe stimulus was selected from a number of stimuli such as oriented colored bars so that it elicited robust activity when presented in the CRF of the cells.

The spatial sensitivity of a single V4 neuron as a function of time is depicted in Figure 2a. Each row in Figure 2a illustrates the temporal evolution of the cell's activity for a different saccade vector. The first three rows show

§To whom correspondence should be addressed (e-mail: andreas.tolias@tuebingen.mpg.de).
‖Present address: Max-Planck Institute for Biological Cybernetics, Spemannstrasse 38, Tuebingen, Germany.
#Present address: Department of Psychology, Princeton University, Princeton, New Jersey 08544.

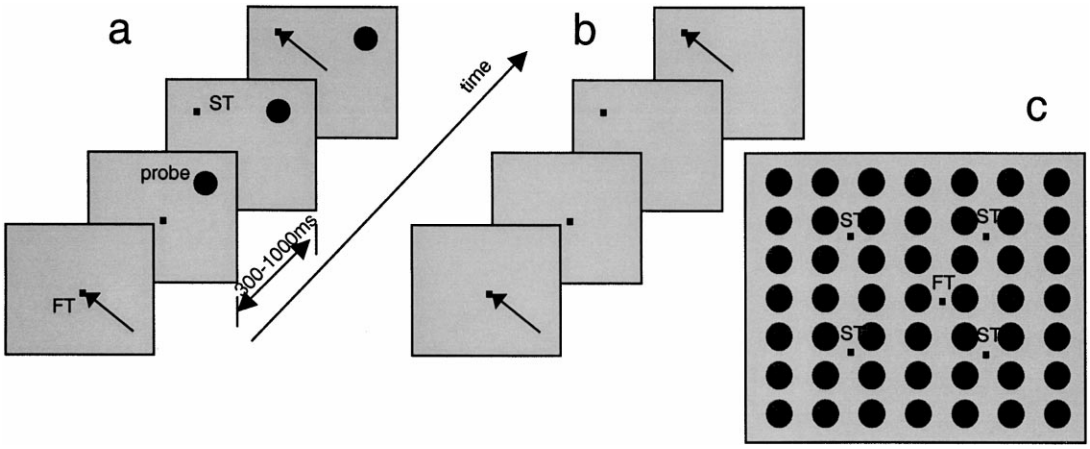

Figure 1. Schematic of the Behavioral Task

Fixation target (FT), saccade target (ST). Arrows represent saccadic eye movements.

(a) Example of a trial where the probe was present.

(b) Example of a trial where no probe appeared.

(c) Example of the various spatial locations the probe was presented (spheres), and the various locations of the saccade target (closed squares). This probe-saccade target arrangement was commonly used. All different trial conditions were randomly interleaved.

the cell's activity for saccade vectors for which there was no visually driven perisaccadic modulation. The neuron initially fires to the appearance of the probe at spatial locations inside its CRF (Figure 2a, second column). Subsequently, the firing rate of the cell decreases as it gradually adapts to the *persistent* probe. The cell starts responding again only after the monkey has foveated the saccade target (Figure 2a, eighth column). This result is not surprising since the probe moves into the receptive field of the neuron as a consequence of the saccade. This postsaccadic-receptive field (postsaccadic-RF, Figure 2a, eighth column) is approximately at the same retinal location as the CRF. No activity above background is seen at the time of the saccade for these particular saccade vectors.

In contrast, for the saccade vector illustrated in the fourth row, the response of the neuron is modulated by the impending saccadic eye movements. While the initial response of the cell to the appearance of the probe is similar to the first three rows, an additional period of increased firing occurs around the time of saccade execution. This perisaccadic activation is dependent on the presence of a visual stimulus (*persistent* probe) and gives rise to a perisaccadic-RF (highlighted by the red square: Figure 2a, row 4, column 6). This perisaccadic-RF is different from the CRF in that it is smaller and its center is closer to the saccade target than is the center of the CRF. In addition, the perisaccadic activation occurs only for specific saccade vectors.

In order to illustrate the characteristics of neuronal firing, we have included spike raster plots for three probe locations. The response of the neuron to the abrupt appearance of the probe at the spatial peak of its CRF is shown in Figure 2b. Figures 2c and 2d demonstrate its response around the time of saccade execution at the spatial peak of the perisaccadic-RF aligned to saccade target onset and saccade onset, respectively. In this case, the neuron starts responding $\sim$50 ms before the eye movement. The black histogram shows the baseline activity when no probe is present. Since the cell does not respond to the execution of the saccade in the absence of the visual probe, the observed perisaccadic activity is not simply due to the saccade per se. Instead, it also requires the concurrent presence of a visual probe indicating that the perisaccadic activation is dependent on the presence of visual stimulation. Figure 2e shows the postsaccadic response of the neuron.

Population Analysis of Perisaccadic Activity

The perisaccadic effects observed in the single cell example were also present in a significant fraction of the population of the neurons studied. From a total of 90 neurons (52 from monkey D and 38 from monkey K), 80 were visually responsive (47 from monkey D and 33 from monkey K). Out of these, 37 showed statistically significant change in perisaccadic activity corresponding to 63 saccade vectors (26 cells from monkey D and 11 cells from monkey K). In Figure 3, we show the raw spike data for all saccade vectors for which we find statistically significant change in perisaccadic activity. None of these 63 saccade vectors showed statistically significant change in perisaccadic activity on the trials where no probe was present. Therefore, the change in perisaccadic activity cannot be simply explained by (1) the onset of the saccade target visually driving the cells up to the time of saccade execution or by (2) the mere motor plan for saccade execution. The presence of the visual probe is essential in order to get the perisaccadic activation.

The saccade vectors for which there was a significant change in the perisaccadic activity are not randomly distributed. This is illustrated in Figures 4a and 4b where the distribution of the saccade vectors that show significant perisaccadic activation differs from the vectors that do not show it (Watson U^2 two-sample test; second-order analysis [Zar, 1998], $p < 0.01$). The saccade vectors that exhibit significant perisaccadic activation are preferentially oriented along the direction of a vector

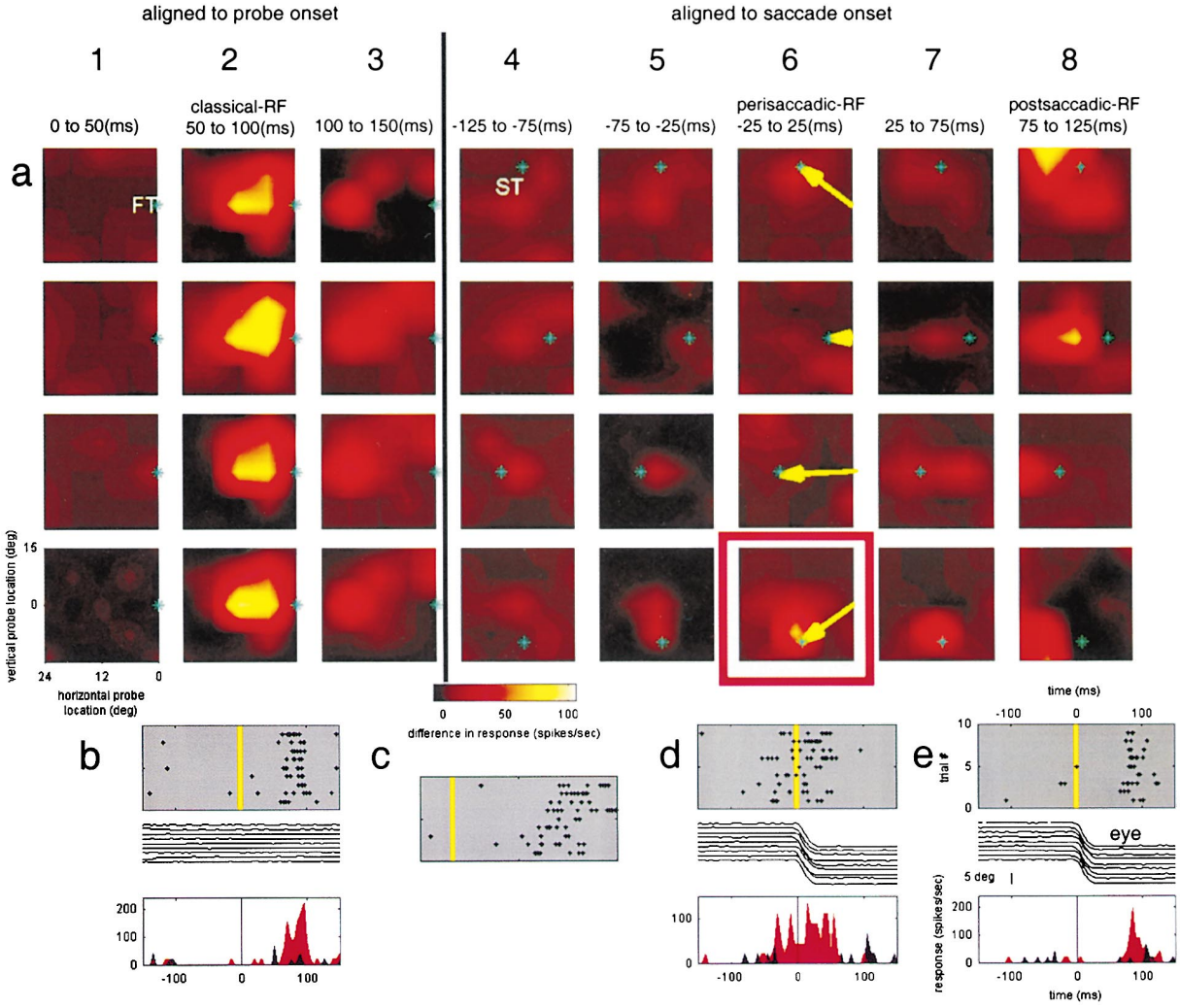

Figure 2. Spatiotemporal Responses of a V4 Neuron

(a) CRF, perisaccadic-RF, postsaccadic-RF, fixation target (FT), and saccade target (ST). The cell's average activity relative to baseline at the various probe spatial locations is shown as color-coded activity maps. These maps are calculated using the interpolation scheme described in the methods (baseline activity is the average response of the neuron when no probe appeared). Along the four rows, from left to right, a series of 50 ms time-bin activity maps are shown. For each row, the saccade target appeared at a different location on the monitor. The blue star within each panel represents both the fixation and saccade targets. The first three columns from the left show the activity of the cell from 0 to +150 ms relative to the onset of the probe while the monkey was fixating on the fixation target. The remaining of the maps show the activity of the cell from −125 to +125 ms relative to saccade execution onset. In the sixth column, the yellow arrows inside the maps pointing to the star (saccade target) schematically represent the saccades.

(b) Response rasters and spike-time histograms (5 ms bin) showing the response of the cell when the probe is located at the spatial peak of the CRF. Horizontal eye movement traces are also shown.

(c) Response rasters show the activity of the neuron at the spatial peak of the perisaccadic-RF. Spikes are aligned to saccade target onset.

(d) Response rasters and red spike-time histogram (5 ms bin) show the activity of the cell when the probe is located at the spatial peak of the perisaccadic-RF (same spikes as in [c]). The black histograms show the activity of the cell when no probe was present (baseline activity). All of these responses are aligned to saccade execution onset as is indicated by the eye movement traces.

(e) Activity at the spatial peak of the postsaccadic-RF.

starting at the fixation target and ending at the center of the CRF of each cell. Moreover, the distribution of the distances from the center of the CRF to the saccade target is different for the saccade vectors that exhibit significant versus nonsignificant perisaccadic activation. Specifically, the saccade vectors that induce significant perisaccadic activation are closer to the CRF by an average of 5° (two-tailed t test: monkey D, $p < 10^{-4}$, and monkey K, $p < 0.01$).

Spatial Relation of CRF and Perisaccadic-RF

In Figure 5, we plot the CRF and the perisaccadic-RF for ten cells (five from each monkey) in order to illustrate their spatial relationship. The blue traces represent the CRF of each neuron and the red traces their corresponding perisaccadic-RF. Note that the perisaccadic-RF tends to be smaller than the CRF and closer to the saccade target.

We quantified the spatial relationship between the

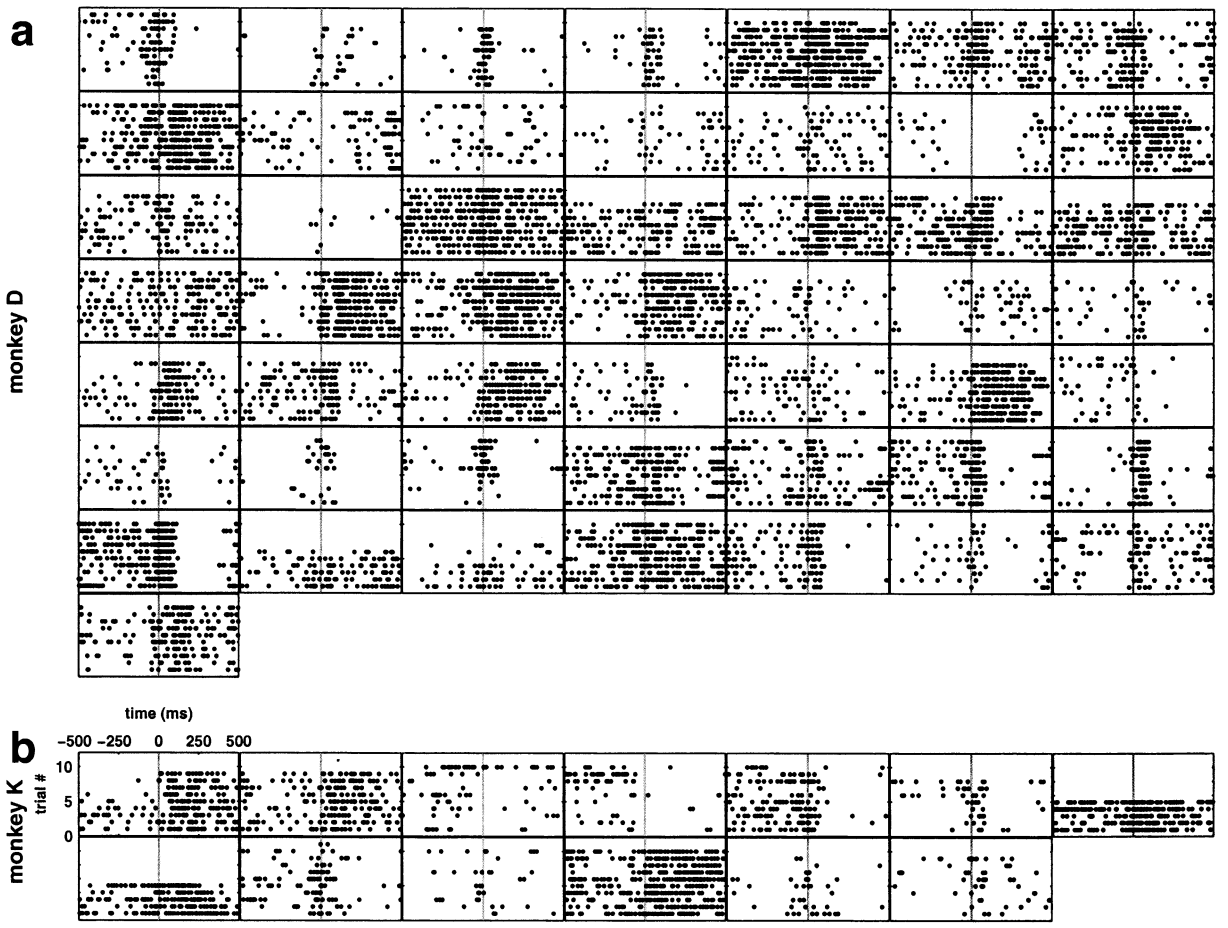

Figure 3. Raster Plots Showing Perisaccadic Activity

Raster plots for all cells recorded from monkeys D and K for which we found significant change in perisaccadic activity (ANOVA followed by Fisher post-hoc test, significant levels were set at $\alpha = 0.05$; see Experimental Procedures).

(a) 50 saccade vectors corresponding to 26 cells for monkey D.

(b) 13 saccade vectors corresponding to 11 cells for monkey K.

All raster plots are aligned to saccade onset (time 0). The size of the fixation window was $<1°$. The monkeys' fixation variability (standard deviation) was: $\sigma_x = 0.21°$, $\sigma_y = 0.23°$ for monkey D and $\sigma_x = 0.17°$, $\sigma_y = 0.18°$ for monkey K. The saccade window was $<2°$. The mean accuracy of saccade execution under these probe-present conditions was $\mu_x = 0.31°$, $\mu_y = 0.25°$ ($\sigma_x = 0.30°$, $\sigma_y = 0.34°$) for monkey D and $\mu_x = 0.46°$, $\mu_y = 0.43°$ ($\sigma_x = 0.44°$, $\sigma_y = 0.41°$) for monkey K. The mean accuracy of saccade execution under the probe-absent conditions was $\mu_x = 0.22°$, $\mu_y = 0.18°$ ($\sigma_x = 0.19°$, $\sigma_y = 0.19°$) for monkey D and $\mu_x = 0.32°$, $\mu_y = 0.36°$ ($\sigma_x = 0.27°$, $\sigma_y = 0.37°$) for monkey K. In some panels, the perisaccadic activation continues much beyond saccade onset. This can happen in cases where the postsaccadic-RF was activated by the edge of the monitor that was visible during the course of the experiment.

CRF and the perisaccadic-RF for all the saccade vectors that showed significant change in perisaccadic activity and for which the entire perisaccadic-RF could be mapped (Figure 6). The center of the perisaccadic-RFs was found to be on average significantly closer to the location of the saccade target than was the center of the CRFs (Figure 6d, two-tailed paired t test, $p < 10^{-3}$). We also compared the location of the purely presaccadic-RFs, computed from a time bin of -75 to 0 ms relative to saccade onset, and found that these receptive fields are also significantly shifted toward the saccade target as compared to the location of the CRFs (two-tailed paired t test, $p < 0.05$). The size of the perisaccadic-RFs was on average significantly smaller than that of the CRFs (Figure 6e, mean change in diameter was 2.1°, maximum 11.4°, two-tailed paired t test, $p < 0.05$). The perisaccadic-RFs were preferentially shifted relative to the CRFs in the direction of a vector pointing from the center of the CRF to the saccade target (Figure 6c, vectors are not uniformly distributed around the circle, nonparametric Moore test [Zar, 1998, p. 640]: monkey D, $p < 0.05$, monkey K, $p < 0.05$). The mean receptive field shift was 4.3° or 0.4 CRF diameters.

It has previously been reported that neurons in the lateral intraparietal area (Duhamel et al., 1992), the superior colliculus (Walker et al., 1995), and the frontal eye fields (Umeno and Goldberg, 1997) show presaccadic "predictive remapping" of their receptive field. Just prior to the execution of a saccade, the receptive field of these neurons shifts to the location it will occupy after the monkey foveates the saccade target. In V4, we did not find evidence for such "predictive remapping" (Figure 6b, nonparametric Moore test [Zar, 1998, p. 640]: monkey D, $p > 0.5$, monkey K, $p > 0.1$). This is also

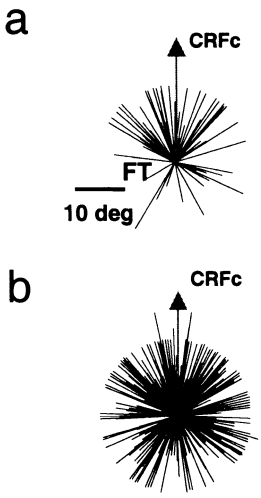

Figure 4. Population Analysis of Direction of Saccade Vectors that Elicit Perisaccadic Activation

(a) The saccade vectors for which there was significant change in perisaccadic activity are plotted relative to the direction of a vector starting at the fixation target and ending at the center of the CRF for each cell. In a few cases, the saccade vectors point away from the CRFs center. This can happen in situations where the CRF is close to the fovea.

(b) The saccade vectors for which there is no significant change in perisaccadic activity are plotted in the same fashion. The distribution of the angles, relative to the horizontal axis, of the saccade vectors showing significant and nonsignificant change in the perisaccadic activity are statistically different (Watson U^2 two-sample test; second-order analysis [Zar, 1998], $p < 0.01$). The significant vectors are more likely to point in the direction of the center of the CRF. Moreover, the distributions of the distances, from the center of the CRFs to the saccade targets, for the saccade vectors that exhibited significant and nonsignificant perisaccadic activation are different. Specifically, the saccade targets for which there is significant perisaccadic activation are closer to the center of the CRF, by an average of 5°, than the ones for which there is no significant perisaccadic activation (two-tailed t test: monkey D, $p < 10^{-4}$, and monkey K, $p < 0.01$).

seen in Figure 5 where green outlines represent the postsaccadic-RFs of the ten illustrated neurons. According to "predictive remapping," the postsaccadic-RFs and the perisaccadic-RFs should be at the same locations. In V4, this is not the case since the postsaccadic-RFs (green outlines) are quite different in size and location from their corresponding perisaccadic-RFs (red outlines).

Temporal Analysis of Perisaccadic Activity

The time course of visual classical activity is compared to the time course of perisaccadic activity in order to demonstrate their differences and show how the perisaccadic activity is related to the execution of the saccade. In Figure 7, we plot the average histograms derived from the 63 raster plots showing neurons that exhibit statistically significant change in perisaccadic activity (Figure 3).

Figures 7a and 7g show the average response functions to the probe flashed at the spatial peak of the CRF relative to probe onset for monkey D and K, respectively. These average population responses have a latency of ~50 ms. For the same neurons as above, we plot in Figures 7b and 7h the average perisaccadic activity profile aligned to the saccade target onset when the probe is located at the spatial peak of the perisaccadic-RF. The latency is now ~100 ms, much longer than the classical response latency. These cells did not display significant perisaccadic activity on the trials where no visual probe was present (Figures 7e and 7k). Therefore, the changes in perisaccadic activity cannot be explained by either visual stimulation due to the saccade target or the mere motor execution of the saccade.

At the same time, however, there is a temporal relationship between the perisaccadic activity and the execution of saccadic eye movements. Specifically, the variability in the time of onset of the perisaccadic activity is smaller the closer it occurs relative to the initiation of the saccade (Figure 8c, Pearson correlation coefficient, $p < 10^{-6}$). In other words, neurons that fire closer to the initiation of the saccade show less variability in their onset of firing than neurons that fire earlier. Such a relationship would not be expected if the perisaccadic activity arose as a purely sensory visual response unrelated to the eye movement. Moreoever, the same neurons show the reverse relation if we analyze their onset of firing in relation to the onset of the saccade target. In this case, the variability in the time of onset of the perisaccadic activity is larger the closer it occurs relative to the onset of the visual saccade target (Pearson correlation coefficient, $p < 0.005$). This result is opposite from what we find for classical visual neuronal activity, where neurons that fire closer to the onset of the visual stimulus show less variability in the time of onset of their firing across identical stimulus presentations (Pearson correlation coefficient, $p < 0.005$). Furthermore, over the population of cells showing significant perisaccadic activation, neuronal latencies across individual trials were correlated with saccade reaction times (Pearson correlation coefficient, $p < 0.05$).

We calculated the neuronal latencies relative to saccade initiation of individual trials using a statistical change-point estimation method for cases where perisaccadic activity was present (Commenges and Seal, 1985). The mean neuronal latency of the perisaccadic activity across trials and neurons was −26 ms (standard deviation 22 ms), with a range from −91 to 17 ms relative to the saccade onset (Figure 8). The variability in the onset of the perisaccadic activity was not correlated with the classical response latency of the cells ($p > 0.3$, Pearson correlation coefficient).

Discussion

The receptive fields of V4 neurons just prior to the initiation of visually guided saccades are smaller than their CRFs and shifted in location toward the saccade goal. This result appears to be intimately related to saccade execution since there is a nontrivial relationship between the onset of perisaccadic activity and the saccade onset (see Results: Temporal Analysis of Perisaccadic Activity). Therefore, the perisaccadic activity is not merely the result of exogenous attentional shifts such as those that take place during the sudden onset of a visual stimulus (Remington et al., 1992).

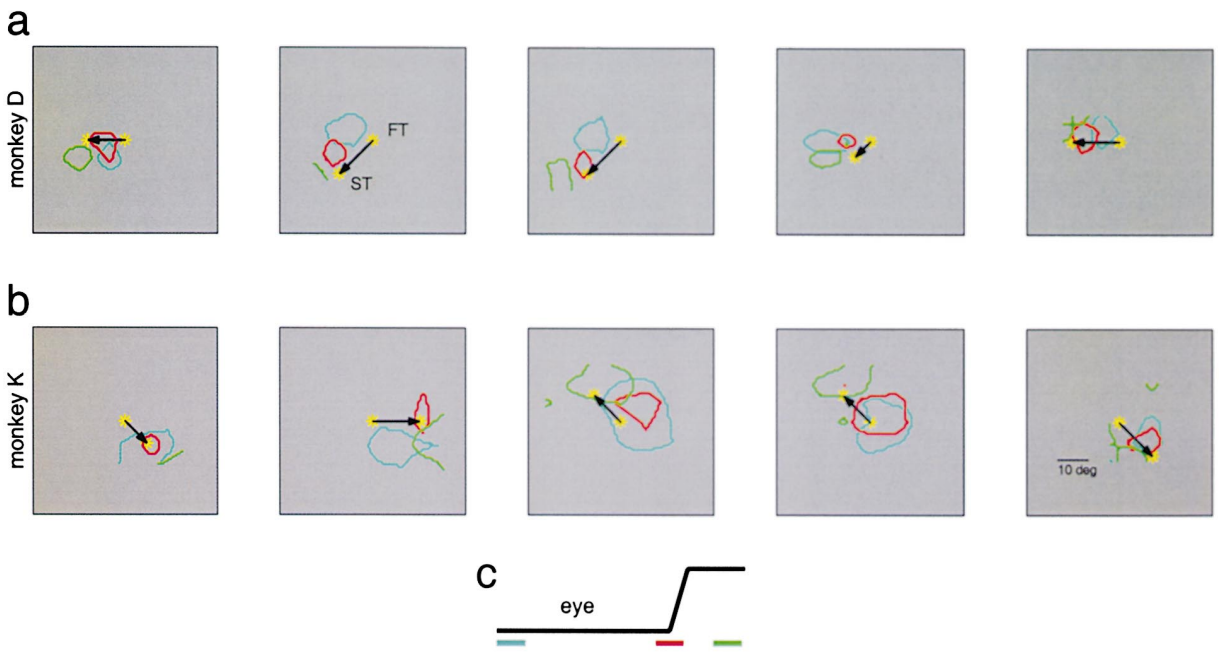

Figure 5. Location of CRF and Perisaccadic-RF

Spatial relation of CRF and perisaccadic-RF for ten neurons (five from each monkey). Fixation target (FT), saccade target (ST).
(a and b) In each plot, the edges of the CRF (shown in blue), the perisaccadic-RF (shown in red), and the postsaccadic-RF (shown in green) are plotted for five cells from each monkey. Some postsaccadic-RFs are not fully mapped as they extend beyond the confines of the monitor.
(c) The time-bins at which the CRF (50–100 ms relative to probe onset), perisaccadic-RF (−25 to 25 ms relative to saccade onset), and postsaccadic-RF (75–125 ms relative to saccade onset) were calculated are shown schematically relative to the eye trace.

The responses of neurons in V4 are known to be modulated by attention (Moran and Desimone, 1985; Haenny et al., 1988; Motter, 1993; Connor et al., 1996; Connor et al., 1997; McAdams and Maunsell, 1999). In particular, during covert attentional tasks the response profile of V4 neurons is shifted toward the focus of attention (Connor et al., 1997). In our experiments, the monkeys were not trained to attend to the visual probe but were simply required to follow the fixation point. It appears then that, in V4, the execution of visually guided saccades is sufficient, but not necessary, for such receptive field modulations to take place. The qualitative agreement between our results and those of voluntary attentional shift experiments suggests a physiological link between covert attentional shifts and visually guided saccadic eye movements in V4.

The strength of attentional modulation effects in V4 depends on the location of the attentional target (Connor et al., 1997). Specifically, Connor and colleagues elegantly demonstrated that, during covert attentional shifts, the receptive field of neurons in V4 does not shift equally in all directions from their CRF center. In our experiments, the modulation of the spatial sensitivity profile of V4 cells occurs preferentially for particular saccade vectors (Figures 4a and 4b). We find that the saccade vectors that exhibited significant perisaccadic activation were on average closer to the center of the CRFs compared to the saccade vectors that did not show significant perisaccadic activation. However, there appear to be exceptions, i.e., saccade vectors that were close to the CRFs but yet showed no significant perisaccadic activation. This asymmetry in receptive fields shifts could reflect asymmetric receptive field shifts similar to Connor and colleagues (Connor et al., 1997). Another possibility is that the asymmetric receptive field shifts could be due to the relationship of the detailed shape of the CRF (and not only its center) to the direction of the saccade, particularly since the CRF itself is not radially symmetric.

The saccade-related receptive field modulations we report here could represent a physiological correlate for a number of psychophysical observations in humans. For example, perceptual identification of letters improves prior to the onset of eye movements when they are placed near the saccadic goal (Kowler et al., 1995). Our result that the sensitivity profiles of V4 neurons shrink and shift toward the saccade target may provide the physiological substrate that underlies presaccadic perceptual enhancement. This perceptual enhancement may reflect a shift in attention preceding saccadic eye movements (Posner, 1980; Mackeben and Nakayama, 1993; Hoffman and Subramaniam, 1995; Kowler et al., 1995).

Another psychophysical observation that may relate directly to our results is the report that near the time of execution of a saccade, human subjects spatially mislocalize abruptly appearing visual stimuli (Cai et al., 1997; Ross et al., 1997). The change in the spatial sensitivity of V4 neurons around the time of the saccade can change the magnification factor of the representation of space in V4 and could account for this behavioral phenomenon.

The change in the spatial sensitivity of cells around the time of initiation of a visually guided saccade might serve at least two purposes. First, it may be part of the neuronal process for selecting possible saccade

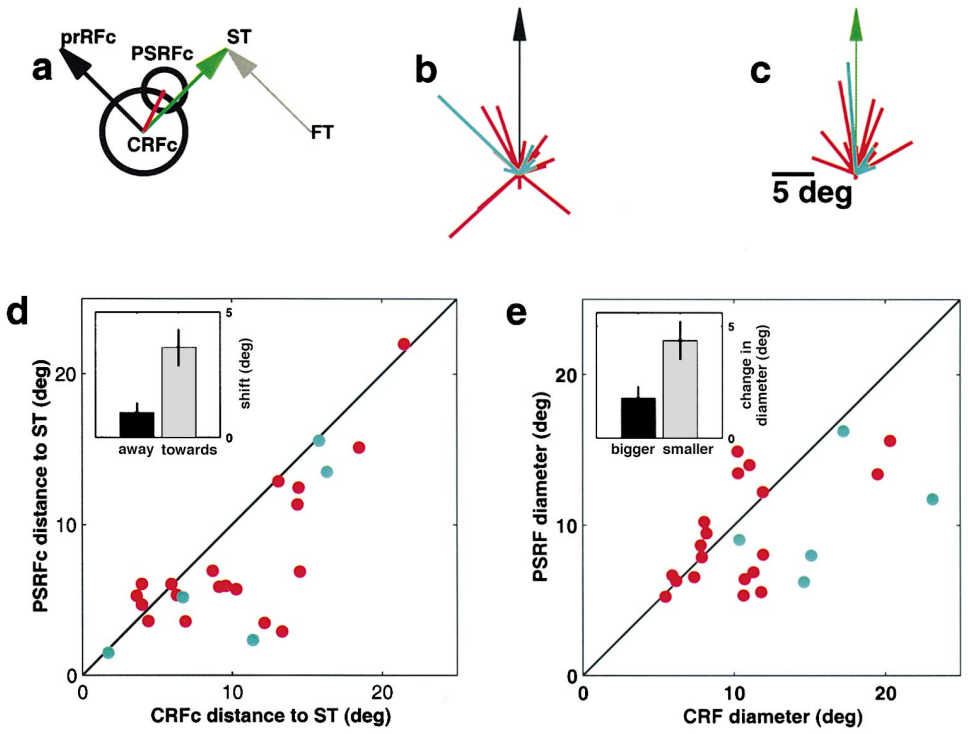

Figure 6. Population Analysis of the Relation between the CRF and the Perisaccadic-RF

Red and blue colored points and lines correspond to monkeys D and K, respectively.

(a) Schematic diagram showing spatial relationships of the CRF, perisaccadic-RF, and saccade target (ST). Fixation target (FT), center of CRF (CRFc), center of perisaccadic-RF (PSRFc), center of hypothetical predictive remapped receptive field (prRFc). Note that the FT-ST (gray) and the CRFc-prRFc (black) vectors are parallel to each other and of the same magnitude.

(b) The black vector indicates the direction of the CRFc-prRFc vector. Each red and light blue line represent receptive field shifts, that is, the CRFc-PSRFc vectors. We show receptive field shifts for saccade vectors that showed a significant change in their perisaccadic activity and for which we could map the entire perisaccadic-RF. The distribution of CRFc-PSRFc vectors relative to the CRFc-prRFc direction is uniformly distributed around the circle (nonparametric Moore test [Zar, 1998, p. 640]: monkey D, $p > 0.5$, monkey K, $p > 0.1$).

(c) The same vectors as in Figure 6b are plotted relative to the CRFc-ST direction, which is the green vector. The distribution of CRFc-PSRFc vectors relative to the CRFc-ST direction is not uniformly distributed around the circle (nonparametric Moore test [Zar, 1998, p. 640]: monkey D, $p < 0.05$, monkey K, $p < 0.05$). The mean of the magnitude of these CRFc-PSRFc vectors is 4.3° or 0.4 CRF diameters degrees.

(d) For the same saccade vectors as above, the distances between the saccade target and the center of gravity of the CRF and the perisaccadic-RF are plotted on the abscissa and the ordinate, respectively. The population is shifted significantly below the diagonal line (two-tailed paired t test, $p < 10^{-3}$). Insert shows means and standard error of the means of shifts for the cases where the perisaccadic-RF was further away from the ST (black bar), and closer to the ST (gray bar), than was the CRF.

(e) The sizes of these CRFs and perisaccadic-RFs are plotted. The population is shifted significantly below the diagonal line (two-tailed paired t test, $p < 0.05$, mean decrease 2.1° in diameter). Insert shows mean and standard error of the mean of size difference for the cases where the perisaccadic-RF was bigger (black bar) and smaller (gray bar) than the CRF.

targets. The decision of choosing saccade endpoints often involves the "high level" perceptual system. This is demonstrated while scanning the image of a face, where the fixation points are "attracted" by high level features such as the eyes, the mouth and the nose (Yarbus, 1967) (Figure 9a). These and other results (Dimitrov et al., 1976) show that the neuronal networks involved in locating interesting points for potential foveation must be capable of computing "high level" perceptual attributes of the visual scene. Area V4 may be part of such a network since it has neurons sensitive to visual attributes (Tanaka et al., 1986; Desimone and Schein, 1987) and provides a major input to the temporal lobe. Furthermore, in our study we show that before the initiation of a saccade, neurons in V4 exhibit spatial sensitivity profiles that result in "emphasizing" the space surrounding future foveation goals (Figures 9b and 9c). This could serve to extract visual attributes needed for saccade target selection. The time of these computations, relative to the onset of eye movements, may be reflected in the beginning of the perisaccadic activation, which in V4 ranged from −91 to 17 ms relative to saccade onset. This range is similar to results reported from other brain areas such as the frontal eye fields (Hanes et al., 1995; Umeno and Goldberg, 1997) that may also be involved in deciding where to look next. Finally, a second possibility is that the perisaccadic-RF modulations may be used to get a head start in processing the next "interesting" set of items, before the fovea lands on them (Henderson et al., 1989; Kowler et al., 1995). Such a mechanism could speed the analysis of these stimuli after foveation.

Experimental Procedures

Recording

We recorded the neural activity from two hemispheres (one left from monkey K and one right from monkey D) of two behaving macaque monkeys (*Macaca Mulatta*). The recording sites from the two hemi-

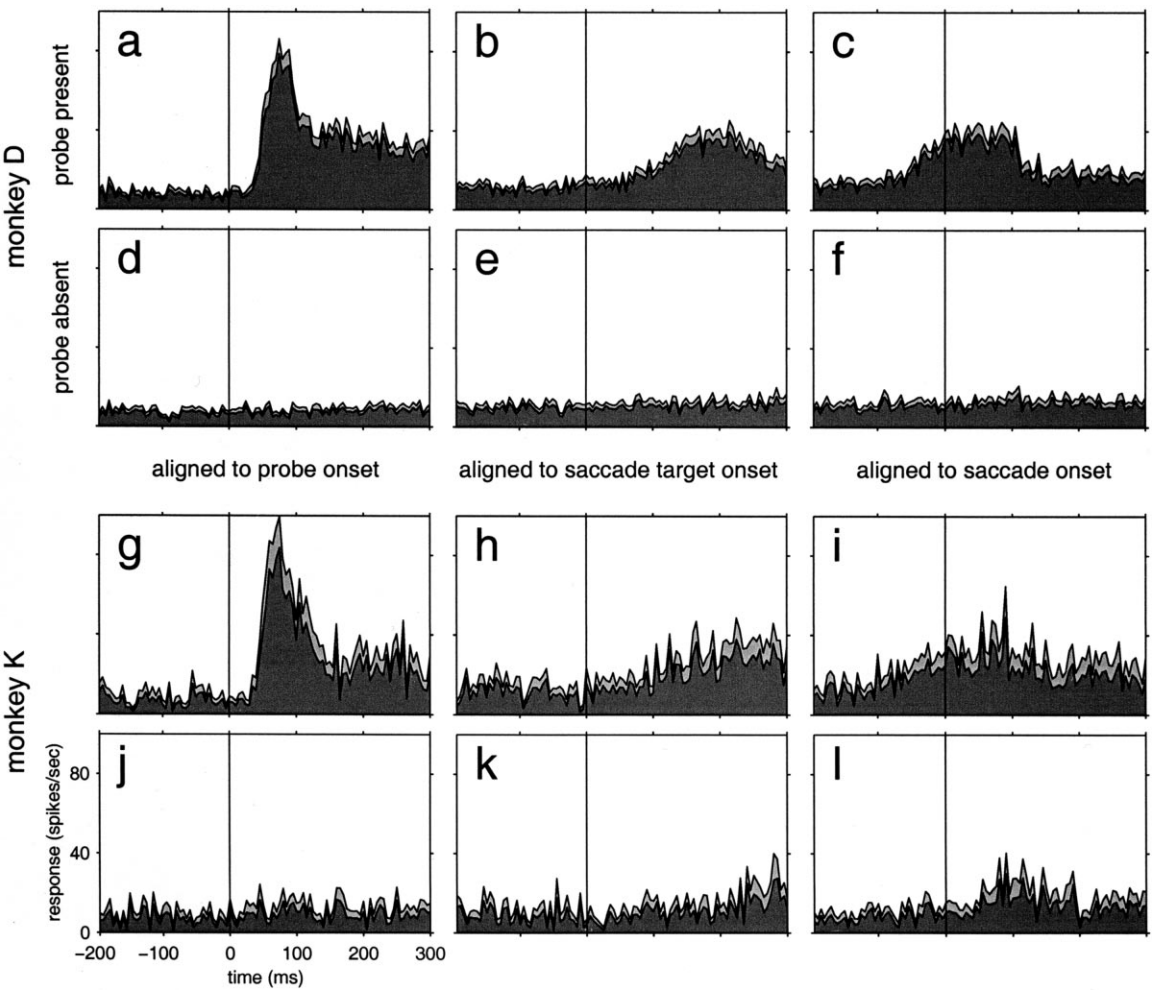

Figure 7. Neuronal Activity Histograms

Mean response profiles of classical and perisaccadic population activity in V4. Standard error of the mean shown as light gray shaded area. Within each panel, spikes are aligned to the solid vertical line.

(a, b, and c) The histograms (5 ms bins) show the average activity for those cells that showed a significant change in perisaccadic activity in monkey D (26 cells, 50 saccade vectors, Figure 3a). The spikes in (a) are aligned to probe onset when the probe was located at the spatial peak of the CRF. In (b) and (c), the spikes are aligned to saccade target onset and saccade execution onset, respectively, with the probe located at the spatial peak of the perisaccadic-RF.

(d, e, and f) These histograms (5 ms bin) show the average activity under the same saccade target location conditions as the ones above but without the presence of the probe (baseline activity). The spikes are aligned correspondingly in the same way.

(g, h, i, j, k, and l) Same as above but for monkey K (11 cells, 13 saccade vectors, Figure 3b).

spheres were in similar anatomical locations as determined by the locations and sizes of the CRFs. Surgical procedures for stainless steel cranial head post, scleral eye coil, and stainless steel recording chamber have been described previously (Logothetis and Schall, 1990; Tehovnik and Lee, 1993). The monkeys were provided for in accordance with the National Institutes of Health Guide for the Care and Use of Laboratory Animals and the guidelines of the Massachusetts Institute of Technology Committee on Animal Care. Neural activity was sampled at 32 kHz, digitized, and stored. Single units were isolated by off-line clustering methods (Data Wave Technologies). Eye movements were sampled at 200 Hz, digitized, and stored for offline analysis.

Visual Stimulation and Behavioral Task

Visual stimuli were displayed on a computer monitor screen 34 cm wide and 27 cm high placed at a distance of 32 to 47 cm from the monkeys eyes (i.e., typical size of monitor 42° horizontal and 36° vertical). The monitor was driven by a TIGA-compatible video board (resolution 1024 by 768 pixels) at 60 Hz refresh rate. The fixation and saccade targets were colored square stimuli 0.3° in diameter. The probe stimuli were larger (~4°) and more salient than the saccade targets, such as oriented colored bars and rendered images of objects such as apples. Each trial began with the appearance of a square fixation target in the center of the monitor in front of the monkey. After the monkey acquired fixation, a probe was flashed at a location chosen randomly from a predetermined set of 16 to 49 positions (median 25 positions). The centers of the probe stimuli were spaced ~6° apart. These parameters were appropriate for optimizing the sampling of the cells' CRF and also covering an area surrounding it within the limitations of how many correct trials our monkeys could run each day (typically 2500 correct trials). A probe was selected so as to activate the cell we recorded from, when presented in its CRF. In contrast, the saccade targets typically evoked very weak responses even when they were presented within the cell's CRF. Once the probe appeared, it remained on until the end of the trial. Following a delay of 300 to 1000 ms, the saccade target appeared on the monitor. For half of the recording sessions, this delay was chosen randomly for each trial (300–1000 ms), while

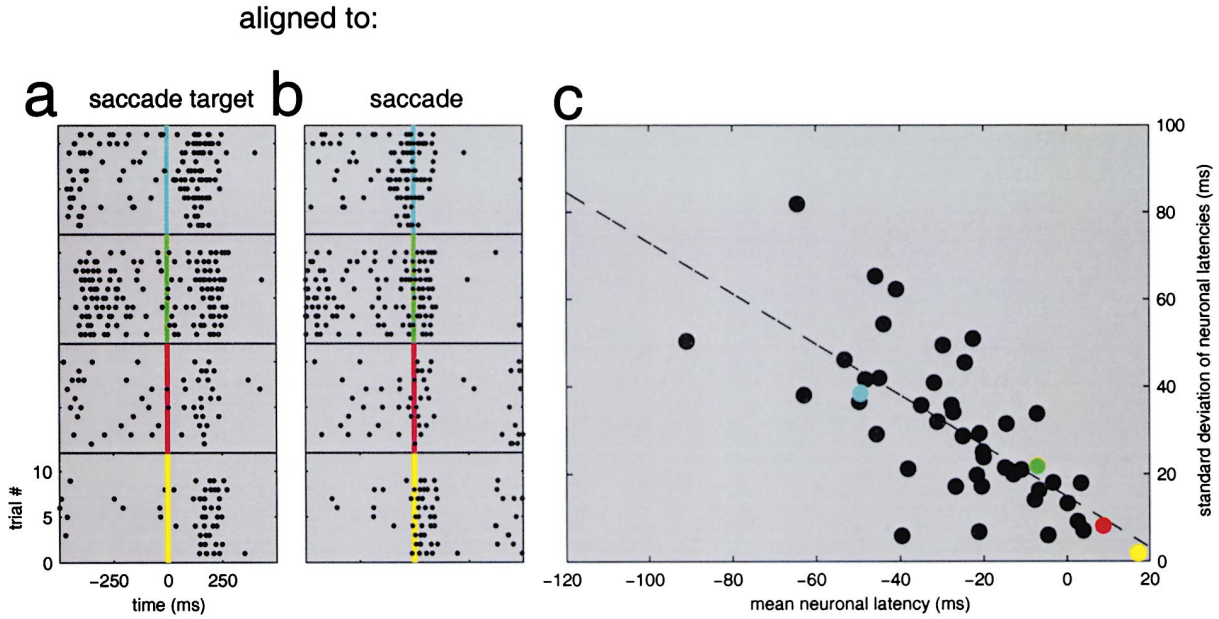

Figure 8. Temporal Analysis of Perisaccadic Activity and Its Relationship to Saccade Initiation

(a) Four raster plots are shown of cells recorded from monkey D for which we found significant perisaccadic activation. All raster plots are aligned to saccade target onset (time 0) indicated by a different colored line for each cell.

(b) Same raster plots as in (a) but aligned to saccade onset (time 0). Note that the closer the onset of activity is to the saccade the better aligned it is across the rasters. By contrast, the closer it occurs with respect to the presentation of the saccade target (a), the less aligned it is across rasters (for instance, compare yellow with blue cell). This is the opposite of what would be expected from a purely sensory visual response.

(c) For each cell from monkey D, which showed significant perisaccadic activation, we computed the neuronal latency of the perisaccadic activity relative to saccade initiation for each trial (see Experimental Procedures). The mean of these neuronal latencies across identical trials is plotted on the abscissa and their standard deviation on the ordinate. Over the population of the cells showing significant perisaccadic activation, the mean latency is strongly correlated with its standard deviation ($p < 10^{-6}$, Pearson correlation coefficient). The yellow, red, green, and blue dot represent the cells shown in (a) and (b). On the abscissa, the distribution of the mean neuronal latency of the perisaccadic activity across neurons is shown. The mean neuronal latency is 26 ms (standard deviation = 22 ms) prior to saccade onset.

for the rest of the recording sessions it was fixed across trials (500 ms). The saccade target location was chosen randomly from a predetermined set of four to eight saccade target locations. Simultaneously with the appearance of the saccade target, the fixation target disappeared. The monkey was rewarded for making a saccadic eye movement to the saccade target. Trials were randomly interleaved. There were around ten identical repetitions for each trial during the course of an experiment.

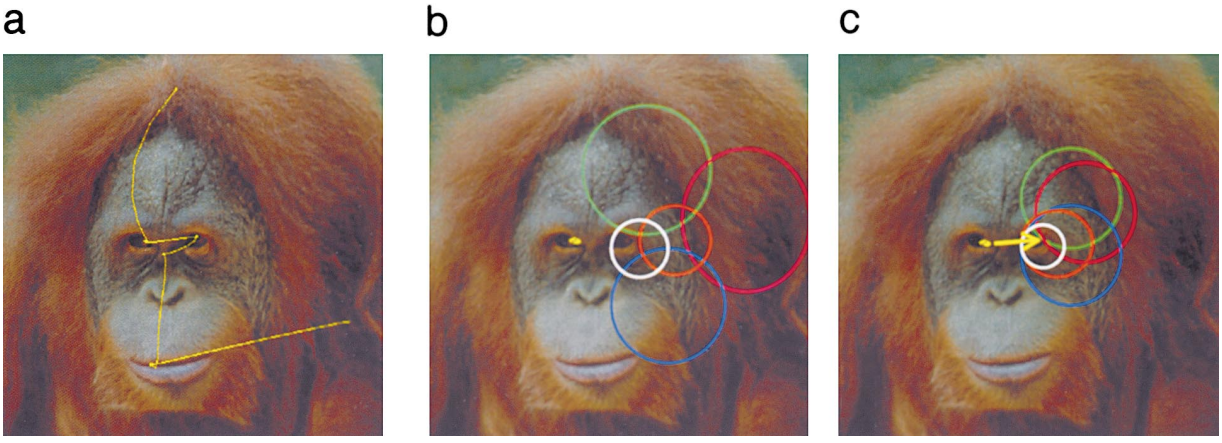

Figure 9. Schematic of Receptive Field Changes that May Occur during Natural Vision

(a) Eye movements (yellow) of a monkey free viewing the underlying orangutan's face.

(b) Schematic of receptive fields during fixation (yellow spot).

(c) Schematic of receptive fields, of the same hypothetical cells as in (b), just before initiation of a saccade towards the left eye of the orangutan.

Analysis

We defined neurons as visually responsive if their firing rate changed significantly to the onset of the probe for at least one probe location. Statistical significance was assessed as follows. We defined two time bins relative to the onset of the probe (time 0): $-205 \leq t_1 < -115$, $50 \leq t_2 < 140$. Let $r^t_{i,\tau}$ denote the firing rate of the neuron during time period t for trial τ and probe location i. We carried out an analysis of variance (ANOVA) with one between factor (activity at different probe locations, i, with as many levels as the number of different probe locations), and one within factor (time bin, with two levels t_1 and t_2). When a significant factor interaction was found in the ANOVA, the neuron was defined as visually responsive. The significance level was set at $\alpha = 0.05$.

We used the same method to find the saccade vectors for which there was a significant change in perisaccadic activity. The two time bins used relative to the onset of the saccade were: $-270 \leq t_1 < -180$, $-50 \leq t_2 < 40$. An ANOVA was carried out with one between factor (activity at different trial types with probe present, with as many levels as the number of different probe locations times the number of saccade vectors), and one within factor (time bin, with two levels t_1 and t_2). When a significant factor interaction was found in the ANOVA, it was followed by Fisher post-hoc tests (Carmen and Swanson, 1973). For each saccade vector, we identified the probe location that gave the maximum perisaccadic activation. After the median firing rate across trials was calculated:

$$R^t_j = median[r^t_{i,\tau}]^N_{\tau=1},$$

we identified the location, i_{max}, of the probe that maximizes $R^{t_2}_j - R^{t_1}_j$, i.e.,

$$i^{2,1}_{max} = \arg\max_i(R^{t_2}_j - R^{t_1}_j).$$

Then we performed the Fisher post-hoc test for the distribution,

$$\left(r^{t_2}_{\substack{2,1\\ i_{max},\tau}} - r^{t_1}_{\substack{2,1\\ i_{max},\tau}}\right), \tau = 1.....N.$$

We assessed a statistically significant change in perisaccadic activity if the mean of the distribution

$$\left(r^{t_2}_{\substack{2,1\\ i_{max},\tau}} - r^{t_1}_{\substack{2,1\\ i_{max},\tau}}\right), \tau = 1.....N$$

is statistically different from zero (Fisher post-hoc test). All significant levels were set at $\alpha = 0.05$. Note that since the response latency of V4 neurons is greater than 40 ms (Figures 7a and 7g), the perisaccadic time bin as defined is guaranteed not to be the result of the change in visual flow the retina sees during the saccade.

Saccade vectors for which there was a significant change in perisaccadic activity when no probe was present were excluded from the analysis. These trials, j, were assessed for the existence of change in the perisaccadic activity if the distribution

$$\left(r^{t_2}_{j,\tau} - r^{t_1}_{j,\tau}\right), \tau = 1.....N$$

was statistically different from zero (two-tailed t test, $p < 0.05$).

We defined the CRF, perisaccadic-RF, and postsaccadic-RF as follows. The average firing rate over trials at each visual probe location was used to construct 50 ms bin data matrices relative to both the onset of the probe and the onset of the saccade. The resulting matrices of raw data were converted with linear interpolation of seven additional points between every sample (e.g., from 5 by 5 to 33 by 33) to activity maps such as the ones color-coded in Figure 2. The following time bins were used: 50 to 100 ms relative to probe onset for the CRF, −25 to 25 ms relative to saccade execution for the perisaccadic-RF, and 75 to 125 ms relative to saccade execution for the postsaccadic-RF. The size of the receptive field was defined to be the area for which the response was equal to or greater than half the maximum response. The center of gravity for this area was then calculated. The trace plots in Figure 5 were computed using the same half-maximum scheme.

The eye movements during trial conditions where perisaccadic activation was present were compared with ones where it was absent for all the cells exhibiting significant perisaccadic activation. The instantaneous horizontal and vertical components of eye movement velocities for these two types of trials were indistinguishable during fixation. The difference between the two means of the velocity profiles (sampled at 200 Hz) was well within one standard error of the mean. The time of the saccade onset was defined as the time when the speed of the eye movements was above a certain threshold. This threshold was fixed for each experiment and was varied across different experiments between 150° and 200° per second.

Neuronal latencies were computed trial by trial (Commenges and Seal, 1985) relative to saccade target onset. Neuronal latency is defined as the point where a response in the spike train is detected, and it was computed using an algorithm described by Commenges and Seal (1985). For each neuron and for identical trials, the neuronal latencies and saccade reaction times were normalized by subtracting their means across these trials. We then computed the correlation between neuronal latencies across individual trials and saccade reaction times (see Results: Temporal Analysis of Perisaccadic Activity).

Acknowledgments

We thank P. Dayan, K. Fuchs Tolias, T. S. Lee, N. K. Logothetis, M. Mehta, G. Rainer, N. Sigala, and W. Slocum for many stimulating discussions and critically reading this manuscript. We also thank W. Slocum for help with computer programming.

Received June 27, 2000; revised December 22, 2000.

References

Andersen, R.A., and Mountcastle, V.B. (1983). The influence of the angle of gaze upon the excitability of the light-sensitive neurons of the posterior parietal cortex. J. Neurosci. *3*, 532–548.

Blatt, G.J., Andersen, R.A., and Stoner, G.R. (1990). Visual receptive field organization and cortico-cortical connectins of the laterla intraparietal area (area LIP) in the Macaque. J. Comp. Neurol. *299*, 421–445.

Boch, R., and Goldberg, M.E. (1989). Participation of prefrontal neurons in the preparation of visually guided eye movements in the rhesus monkey. J. Neurophysiol. *61*, 1064–1084.

Boussaoud, D., Desimone, R., and Ungerleider, L.G. (1991). Visual topography of area TEO in the macaque. J. Comp. Neurol. *306*, 554–575.

Cai, R.H., Pouget, A., Schlag-Rey, M., and Schlag, J. (1997). Perceived geometrical relationships affected by eye-movement signals. Nature *386*, 601–604.

Carmen, S.G., and Swanson, M.R. (1973). An evaluation of ten pairwise multiple comparison procedures by Monte Carlo methods. J. Am. Stat. Assoc. *68*, 66–74.

Carpenter, R.H.S. (1988). Movements of the Eyes, Second Edition (London: Pion Ltd).

Commenges, D., and Seal, J. (1985). The analysis of neuronal discharge sequences: change-point estimation and comparison of variances. Stat. Med. *4*, 91–104.

Connor, C.E., Gallant, J.L., Preddie, D.C., and Van Essen, D.C. (1996). Responses in area V4 depend on the spatial relationship between stimulus and attention. J. Neurophysiol. *75*, 1306–1308.

Connor, C.E., Preddie, D.C., Gallant, J.L., and Van Essen, D.C. (1997). Spatial attention effects in macaque area V4. J. Neurosci. *17*, 3201–3214.

Desimone, R., and Gross, C.G. (1979). Visual areas in the temporal cortex of the macaque. Brain Res. *178*, 363–380.

Desimone, R., and Schein, S.J. (1987). Visual properties of neurons in area V4 of the macaque: sensitivity to stimulus form. J. Neurophysiol. *57*, 835–868.

Dimitrov, G., Yakimoff, N., Mateeff, S., Mitrani, L., Radil-Weiss, T., and Bozkov, V. (1976). Saccadic eye movements on Bela Julesz' figure. Vision Res. *16*, 411–414.

Dubner, R., and Zeki, S.M. (1971). Response properties and receptive fields of cells in an anatomically defined region of the superior temporal sulcus in the monkey. Brain Res. *35*, 528–532.

Duhamel, J.-R., Colby, C.L., and Goldberg, M.E. (1992). The updating

of the representation of visual space in parietal cortex by intended eye movements. Science *255*, 90–92.

Fischer, R., and Boch, R. (1981a). Selection of visual targets activates prelunate cortical cells in trained rhesus monkey. Exp. Brain Res. *41*, 431–433.

Fischer, B., and Boch, R. (1981b). Enhanced activation of neurons in prelunate cortex before visually guided saccades of trained rhesus monkeys. Exp. Brain Res. *44*, 129–137.

Haenny, P.E., Maunsell, J.H.R., and Schiller, P.H. (1988). State dependent activity in monkey visual cortex. II. Retinal and extraretinal factors in V4. Exp. Brain Res. *69*, 245–259.

Hanes, D.P., Thompson, K.G., and Schall, J.D. (1995). Relationship of presaccadic activity in frontal eye field and supplementary eye field to saccade initiation in macaque: poisson spike train analysis. Exp. Brain Res. *103*, 85–96.

Hartline, H.K. (1940). The receptive fields of optic nerve fibers. J. Physiol. *130*, 690–711.

Henderson, J.M., Pollatsek, A., and Rayner, K. (1989). Covert visual attention and extrafoveal information use during object identification. Percept. Psychophys. *45*, 196–208.

Hikosaka, K. (1998). Representation of foveal visual-fields in the ventral bank of the superior temporal sulcus in the posterior inferotemporal cortex of the macaque monkey. Behav. Brain Res. *96*, 101–113.

Hoffman, J.E., and Subramaniam, B. (1995). The role of visual attention in saccadic eye movements. Percept. Psychophys. *57*, 787–795.

Kowler, E., Anderson, E., Dosher, B., and Blaser, E. (1995). The role of attention in the programming of saccades. Vision Res. *35*, 1897–1916.

Logothetis, N.K., and Schall, J.D. (1990). Binocular motion rivalry in macaque monkeys: eye dominance and tracking eye movements. Vision Res. *30*, 1409–1419.

Mackeben, M., and Nakayama, K. (1993). Express attentional shifts. Vision Res. *33*, 85–90.

McAdams, C.J., and Maunsell, J.H. (1999). Effects of attention on orientation-tuning functions of single neurons in macaque cortical area V4. J. Neurosci. *19*, 431–441.

Moore, T. (1999). Shape representations and visual guidance of saccadic eye movements. Science *285*, 1914–1917.

Moore, T., Tolias, A.S., and Schiller, P.H. (1998). Visual representations during saccadic eye-movements. Proc. Natl. Acad. Sci. USA *95*, 8981–8984.

Moran, J., and Desimone, R. (1985). Selective attention gates visual processing in the extrastriate cortex. Science *229*, 782–784.

Motter, B.C. (1993). Focal attention produces spatially selective processing in visual cortical areas V1, V2, and V4 in the presence of competing stimuli. J. Neurophysiol. *70*, 909–919.

Posner, M.I. (1980). Orienting of attention. Q. J. Exp. Psychol. *32*, 3–25.

Rainer, G., Asaad, W.F., and Miller, E.K. (1998). Memory fields of neurons in the primate prefrontal cortex. Proc. Natl. Acad. Sci. USA *95*, 15008–15013.

Remington, R.W., Johnston, J.C., and Yantis, S. (1992). Involuntary attentional capture by abrupt onsets. Percept. Psychophys. *51*, 279–290.

Robinson, D.L., Goldberg, M.E., and Stanton, G.B. (1978). Parietal association cortex in the primate: sensory mechanisms and behavioral modulations. J. Neurophysiol. *41*, 910–932.

Ross, J., Morrone, M.C., and Burr, D.C. (1997). Compression of visual space before saccades. Nature *386*, 598–601.

Suzuki, H., and Azuma, M. (1983). Topographic studies on visual neurons in the dorsolateral prefrontal cortex of the monkey. Exp. Brain Res. *53*, 47–58.

Tanaka, M., Weber, H., and Creutzfeldt, O.D. (1986). Visual properties and spatial distribution of neurones in the visual association area on the prelunate gyrus of the awake monkey. Exp. Brain Res. *65*, 11–37.

Tehovnik, E.J., and Lee, K. (1993). The dorsomedial frontal cortex of the rhesus monkey: topographic representation of saccades evoked by electrical stimulation. Exp. Brain Res. *96*, 430–442.

Umeno, M.M., and Goldberg, M.E. (1997). Spatial processing in the monkey frontal eye field .1. predictive visual responses. J. Neurophysiol. *78*, 1373–1383.

Walker, M.F., Fitzgibbon, E.J., and Goldberg, M.E. (1995). Neurons in the monkey superior colliculus predict the visual result of impending saccadic eye movements. J. Neurophysiol. *73*, 1988–2003.

Wurtz, R.H. (1969). Visual receptive fields of striate cortex neurons in awake monkeys. J. Neurophysiol. *32*, 727–742.

Wurtz, R.H., and Mohler, C.W. (1976). Enhancement of visual response in monkey striate cortex and frontal eye fields. J. Neurophysiol. *39*, 766–772.

Yarbus, A.L. (1967). Eye Movements and Vision (New York: Plenum).

Zar, J.H. (1998). Biostatistical Analysis, Fourth Edition (Upper Saddle River, NJ: Prentice Hall).